

# Equalisation of precession rates of galactic orbits (Part 3)

S. Edgeworth

First published: 12 May 2013

---

## Abstract

In a disk galaxy, two groups of simple power-law fields are examined. It is proposed that one group of fields produces galactic components with positive ellipticity gradient and retrograde pattern speed, and that the other group of fields produces galactic components with negative ellipticity gradient and prograde pattern speed. Some isophotal examples are referred to.

---

This investigation assumes that in a disk galaxy, each interaction between two adjacent nested galactic orbits, which equalises their precession rates, does so specifically by modifying their orbital ellipticities. The galactic components, which would result in a disk galaxy from that assumed process, were constructed in two different power-law fields (1) (2).

In (1) it was shown that the  $f \propto \sqrt{d}$  field produces a galactic component with negative ellipticity gradient and prograde pattern speed. Here it is provisionally suggested that this result may to some extent be generalised to fields of the form  $f \propto d^x$  in the range  $0.5 \leq x < 1$ . It seems likely that this range of fields may produce galactic components with negative ellipticity gradient and prograde pattern speed, and that, if it is possible for two such components to be nested one within the other, all in the same field, then the inner component will have a faster angular pattern speed than the outer component.

In (2) it was shown that the  $f \propto d^2$  field produces a galactic component with positive ellipticity gradient and retrograde pattern speed. Here it is provisionally suggested that this result may to some extent be generalised to fields of the form  $f \propto d^x$  in the range  $1 < x \leq 2$ . It seems likely that this range of fields may produce galactic components with positive ellipticity gradient and retrograde pattern speed, and that if two such components of this type are nested one within the other, all in the same field, then the outer component will have a faster angular pattern speed than the inner component.

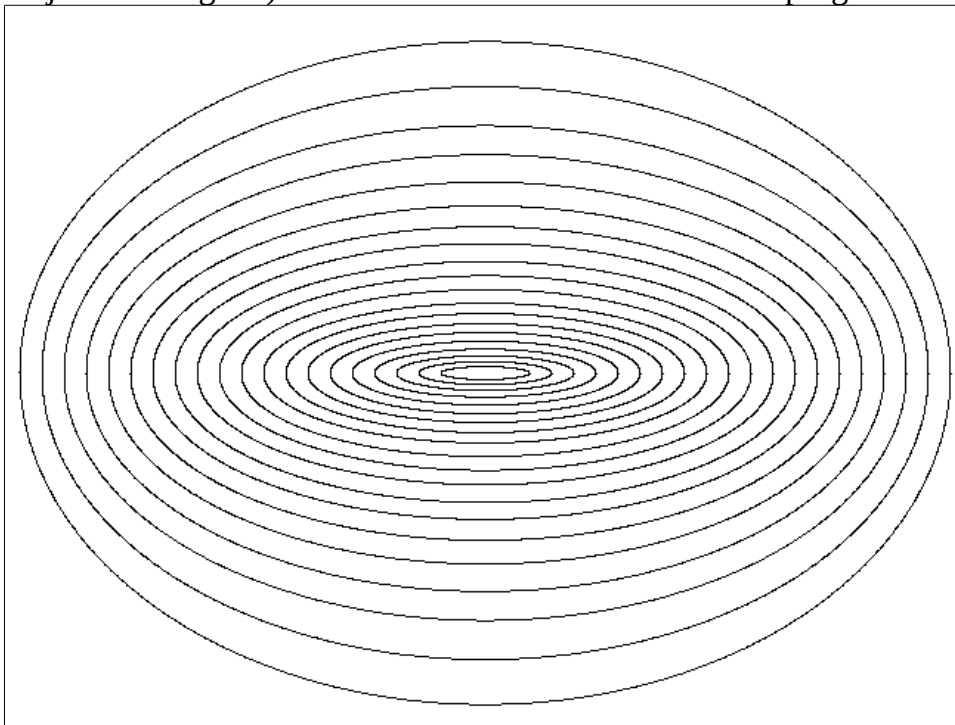
The two ranges of power-law fields proposed above are separated by the  $f \propto d$  harmonic field, which has the remarkable properties that apsidal precession is zero, and orbital period is independent of orbit size and ellipticity (3).

The suggested generalisations are provisional. It is possible that further calculations of the components produced in various specific fields within the above ranges, may prove the generalisations to be partially incorrect.

Although the two ranges of fields have distinctly opposite properties, and produce opposite types of component, kinematic density waves if present would in both cases be usually trailing.

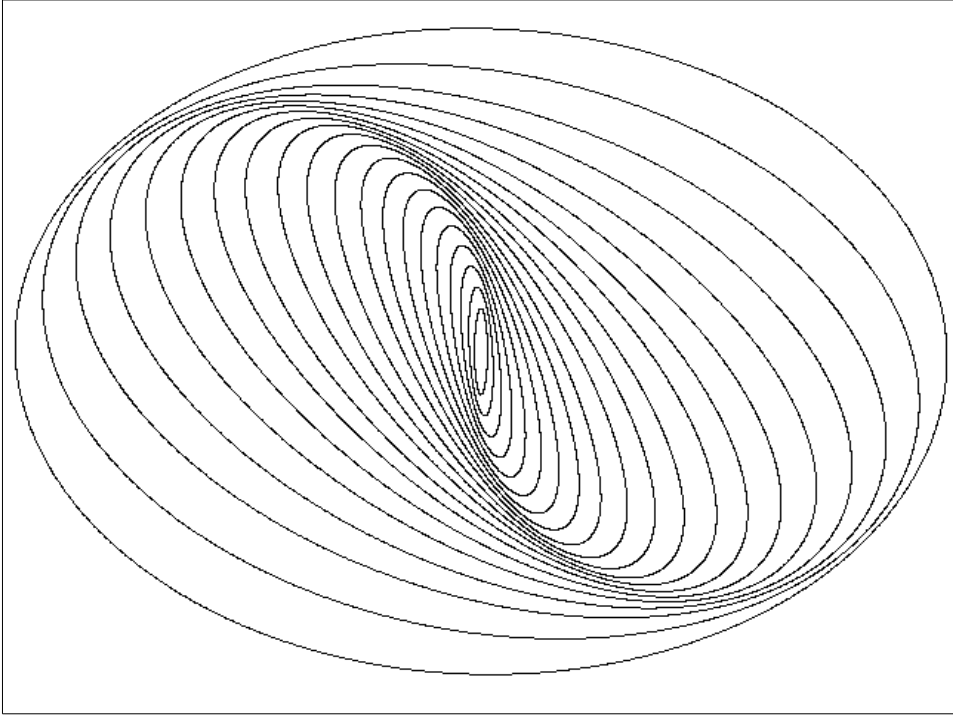
---

**Figure 1:** Galactic component with equalised precession rates in the  $f \propto \sqrt{d}$  field (shown with major axes aligned). Orbits are clockwise. Precession is prograde.



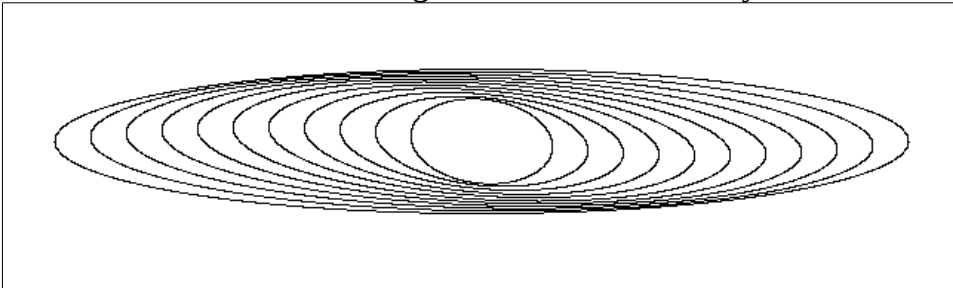
---

**Figure 2:** Galactic component with equalised precession rates in the  $f \propto \sqrt{d}$  field (shown with major axes differentially rotated). Orbits are clockwise. Precession is prograde. Kinematic density waves are trailing.



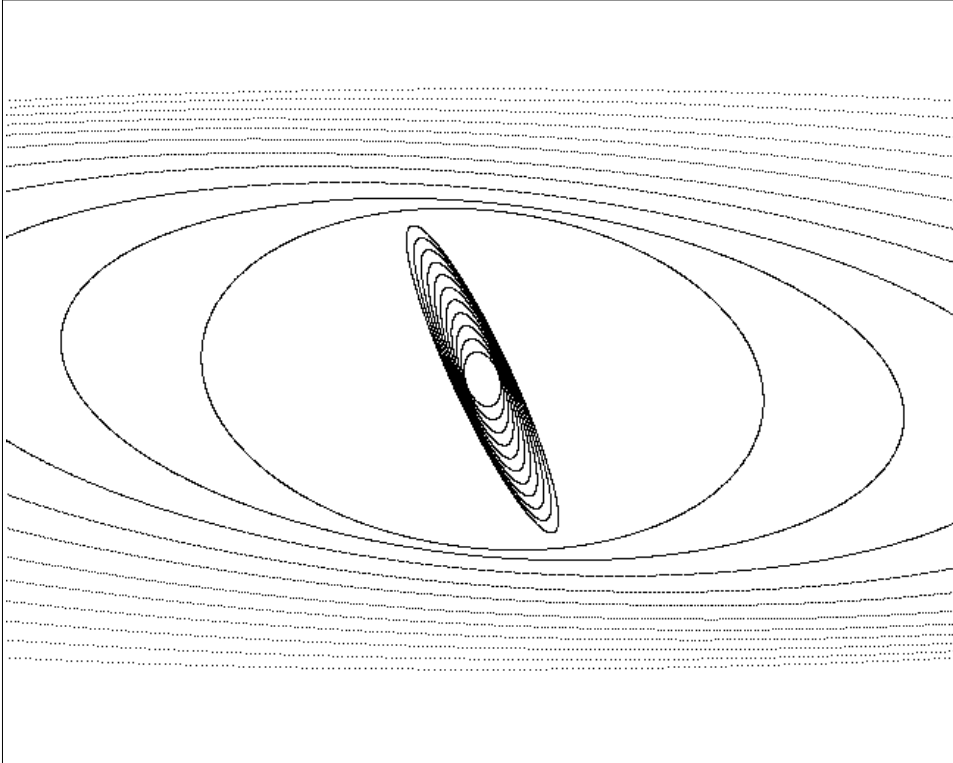
---

**Figure 3:** Galactic component with equalised precession rates in the the  $f \propto d^2$  field. Orbits are clockwise. Precession is retrograde. Kinematic density waves are trailing.



---

**Figure 4:** Two nested self-similar galactic components in the  $f \propto d^2$  field. Orbits are clockwise. Precession is prograde. Kinematic density waves are trailing. The outer component has a faster angular pattern speed than the inner component.



---

Next, a few examples in real galaxies of the two types of component are referred to, in isophotal studies by others. Clearly the fields within which these real components exist are non-axisymmetric, and more complex than a simple power-law field. Therefore the examples are referred to simply to show that components with positive ellipticity gradient, and with negative ellipticity gradient, both may exist in real galaxies.

Examples of components with negative ellipticity gradient:

See Athanassoula, Morin, et al, 1990 (4).

In that work, in figure 3, the right hand column shows deprojected isophotal maps (with the bulge masked out) of NGC 0936, 4314, 4596 and 2787.

In that same work, figure 4 shows deprojected ellipticity graphs of NGC 0936, 1326, 2217, 2787, 2859, 3945, 4314, 4340, 4596, 4371, 6942 and 7155. In each ellipticity graph, the thin solid line includes the bulge contribution, however the heavier line (consisting of symbols) shows the ellipticity graph after the bulge contribution has been masked out.

Examples of components with positive ellipticity gradient:

See Athanassoula, Gadotti, et al, 2009 (5).

In that work , figure 2 shows direct (not deprojected) isophotal maps of NGC 357 and 799. In that same work, in figure 3, in the top image of column 2, the red line shows the deprojected ellipticity graph of NGC 357. And also in figure 3, in the top image of column 4, the red line shows the deprojected ellipticity graph of NGC 799.

## References

(1) Equalisation of precession rates of galactic orbits (Part 1),

<http://www.orbsi.uk/space/research/se/pdf/equalisation-precession-galactic-orbits-1.pdf>

(2) Equalisation of precession rates of galactic orbits (Part 2),

[www.orbsi.uk/space/research/se/pdf/equalisation-precession-galactic-orbits-2.pdf](http://www.orbsi.uk/space/research/se/pdf/equalisation-precession-galactic-orbits-2.pdf)

(3) Blitzer, L.,

Hyper-Elliptic Orbits,

[1988CeMec..42..215B](http://adsabs.harvard.edu/full/1988CeMec..42..215B)

(4) Athanassoula, E., Morin, S., Wozniak, H., Puy, D., Pierce, M. J., Lombard, J.

The shape of bars in early-type barred galaxies

1990MNRAS.245..130A

[adsabs.harvard.edu/full/1990MNRAS.245..130A](http://adsabs.harvard.edu/full/1990MNRAS.245..130A)

(5) Athanassoula, E.; Gadotti, D. A.; Carrasco, L.; Bosma, A.; de Souza, R. E.; Recillas, E.

Barred Galaxy Photometry: Comparing results from the Cananea sample with N-body simulations

2009RMxAC..37...79A

[adsabs.harvard.edu/abs/2009RMxAC..37...79A](http://adsabs.harvard.edu/abs/2009RMxAC..37...79A)

v.1: 12 May 2013.

v.2: 12 May 2013 (improved the generalised ranges of fields).

v.3: 12 May 2013 (added illustrations).

v.4: 30 Nov 2017 (minor wording improvements).